

## Two-site Model for Aluminum Oxide with Mass Balanced Competitive pH+Salt/Salt Dependent Reactions<sup>1</sup>

C. P. SCHULTHESS AND D. L. SPARKS<sup>2</sup>

### ABSTRACT

A backtitration technique was used to collect proton isotherm data for an Al oxide, and was found to be stoichiometrically related to the cation and anion isotherm behavior. The adsorption of various ions by the Al oxide surface was modeled based on: (i) two surface sites, (ii) pH+salt-dependent reactions ( $H^+$  and  $Cl^-$ ,  $2OH^-$ , or  $Na^+$  and  $OH^-$ ), (iii) competitive salt-dependent reactions ( $Na^+$  or  $Cl^-$ ), (iv)  $CO_2(aq)$  pH-dependent reactions with the surface-OH groups, and (v) presence of an unknown  $M^+Cl^-$  salt (0.0005 M). The total number of Al sites was  $1.7 \mu mol m^{-2}$  or  $3.4 \mu mol m^{-2}$  of total available sites. The pH of point of zero salt effect (PZSE) represented the surface condition in which the negative charges (or cation surfaces) equaled the positive charges (or anion surfaces); the cation exchange capacity (CEC) equaled the anion exchange capacity (AEC) at this value. The CEC-AEC data and proton isotherm data were stoichiometrically correlated. The pH of PZSE values ranged from 7.50 to 7.76 depending on the electrolyte concentration present, with lower values as the concentration increased. The negative shifts in the PZSE values are due to anion impurities initially present on the surface and positive shifts are due to cation impurities.

**Additional Index Words:** cation/anion/proton isotherms, competitive reactions, equilibrium constants, mass balanced equations, PZSE, PZNC, ZPC.

Schulthess, C.P., and D.L. Sparks. 1987. Two-site model for aluminum oxide with mass balanced competitive pH+salt/salt dependent reactions. *Soil Sci. Soc. Am. J.* 51:1136-1144.

THE ADSORPTION OF DISSOLVED SUBSTANCES on a solid phase (charcoal) was accidentally discovered in 1785 by J.T. Lowitz (Figurovsky, 1973). A.L. Lavoisier (1743-1794) advanced a chemical, rather than mechanical, theory for the phenomenon of adsorption (Figurovsky, 1973). Modeling of the surface chemistry of oxides, colloids, or soils, has long been recognized by researchers as essential in optimizing crop yields, soil productivity, or the efficiency of any system requiring an interaction with a solid phase. Adsorption models were initially intended to describe gas adsorption by solids, and have been applied with some success to aqueous adsorption. The most fa-

mous contribution was made by Langmuir (1918), whose equation may be easily derived for cation adsorption onto an oxide surface site. Assuming the following surface reaction



where S is the surface of the solid phase, one can then define the corresponding equilibrium constant,  $K$ , as

$$K = \frac{\{SO^-\}(M^+)}{\{SOM\}} \quad [2]$$

The mass balance condition is then

$$\Gamma_{\max} = \{SO^-\} + \{SOM\} \quad [3]$$

where

$$\begin{aligned} \Gamma_{\max} &= \text{total number of sites,} \\ \{SOM\} &= \Gamma_{M^+} = \text{concentration of sites adsorbing } M^+, \\ \{SO^-\} &= \text{concentration of sites lacking } M^+, \text{ and} \\ (M^+) &= c = \text{bulk solution equilibrium concentration of } M^+. \end{aligned}$$

Combining Eq. [2] and [3] gives

$$\begin{aligned} \Gamma_{\max} &= \frac{\{SOM\}}{k(M^+)} + \{SOM\} \\ &= \{SOM\} \left[ \frac{1 + k(M^+)}{k(M^+)} \right] \quad [4] \end{aligned}$$

where  $k = 1/K$ . Rearranging one finds that

$$\frac{\Gamma_{M^+}}{\Gamma_{\max}} = \frac{kc}{1 + kc} \quad [5]$$

Equation [5] is the Langmuir adsorption isotherm, and is often applied to cation and anion adsorption modeling (Olsen and Watanabe, 1957; Huang and Stumm, 1973). The concentration parameters should be expressed as activity values.

If the cation in question is  $H^+$ , the assumption is made that the proton becomes progressively more difficult to remove with each incremental removal of protons or degree of titration (Huang, 1981). Equation [2] is redefined in terms of an intrinsic equilibrium constant

$$K^{\text{int}} = \frac{\{SO^-\}(H^+) \exp(-F\Psi_o/RT)}{\{SOH\}} \quad [6]$$

<sup>1</sup> Published with the approval of the Director of the Delaware Agric. Exp. Stn. as Miscellaneous Paper no. 1172. Contribution no. 215 of the Dep. of Plant Science, Univ. of Delaware, Newark, DE 19717-1303. Received 17 Nov. 1986.

<sup>2</sup> University Graduate Research Fellow and Professor of Soil Chemistry, respectively.

The exponential term in Eq. [6] assumes that the surface charge causes a change in reactivity between the ions at the surface and in the bulk solution, which is described by the Boltzmann distribution (Barrow, 1985). The  $K^{int}$  value is then the acidity constant in a completely chargeless environment (Huang, 1981). Another hypothesis assumes the existence of a porous gel layer with an exponential decay of porosity capable of adsorbing ions (Lyklema, 1968; Romm and Rubashkin, 1985), which also results in an exponential adjustment to the  $H^+$  ion concentration sorbed on the surface. In the presence of a divalent cation, the intrinsic equilibrium constant has been defined as (Barrow, 1985)

$$K^{int} = \frac{[SOM^+](H^+) \exp(-F\Psi_s/RT)}{[SOH](M^{2+}) \exp(-2F\Psi_\beta/RT)} \quad [7]$$

Equation [7] is derived from a multilayer model that assumes the inner layer ( $s$ ) to adsorb  $H^+$  and  $OH^-$  ions, and the second layer ( $\beta$ ) to adsorb the electrolyte ions. It is not clear why the  $H^+$  ion should be treated differently than any other ion. The "correction" in Eq. [6] does allow for exponential fitting of the convex behavior of surface charge vs. pH ( $\sigma_o$ -pH) curves. The assumption of two separate potentials for each layer and corresponding exponential corrections in Eq. [7] also allows for exponential fitting of the  $\sigma_o$ -pH curves. There are many models from which to choose (Barrow, 1985; Westall and Hohl, 1980), and they all fit  $\sigma_o$ -pH curves fairly well. Sposito (1983) observed that "these surface complexation models are *too* successful". However, there is insufficient proof as to which model is more realistic, or as to why the Boltzmann distribution correction term is necessary. Sposito (1984) discusses that equations similar to Eq. [6] should be formulated for metal surface reactions that result in a charged surface; however, he also states that very small or negligible dependence on the exponential terms for metal surface reactions are observed in practice.

Potentiometric titration curves adhere to the principle of electroneutrality that, upon rearrangement of the electroneutrality terms, yields an equation of mass conservation. The  $\sigma_o$ -pH curves are based on the same principle of mass conservation that cation and anion isotherms are based; i.e.,

$$\text{mass adsorbed} = \text{mass added} - \text{mass recovered} \quad [8]$$

Schulthess and Sparks (1986) argued that Eq. [8] has not been properly applied to proton isotherm analyses due to the solubility of the solid phase, which is pH dependent. Applying a backtitration technique, a proton isotherm was obtained that showed maximum adsorption limits, distinct plateaus, and titration breaks. These observations were radical in that the assumptions used for Eq. [6] no longer apply. That is, the proton isotherm is not convex, and does not need to be fitted by exponential correction terms. It is strongly suggested that the exponential term in Eq. [6] is merely tracking the solubility behavior of the solid phase.

The Langmuir isotherm is a special case of the more general mass balanced set of equations; specifically, a single site with only one reaction assumed. In this article, a backtitration analysis of an Al oxide was made with the intention of presenting a proton isotherm

model based on mass balanced equations, without assuming a variable stability constant with increasing degree of titration (i.e.,  $K = K^{int} \exp[F\Psi_o/RT]$  will not be assumed). The objectives of formulating a model were to (i) establish a definition, or interpretation, of the point of zero salt effect (PZSE) value obtained by the backtitration technique (Schulthess and Sparks, 1986), (ii) interpret the effect of the electrolyte concentration on the amount of proton adsorption, and (iii) advance a discussion on the validity of zero point of charge (ZPC) definitions determined through traditional singular reference curve methods (Schulthess and Sparks, 1986).

## MATERIALS AND METHODS

The Al oxide studied was a  $\gamma$ - $Al_2O_3$  made by the Degussa Corp. of Teterboro, NJ, under the name of Aluminum Oxide C<sup>®</sup>. The oxide was acid washed with  $HClO_4$  at pH 4.2, followed by an  $H_2O$  wash. The  $H_2O$  used was purified through an ultrapure D8902 cartridge (Barnstead Co., Newton, MA) and  $N_2$  purged for at least 15 min before each use. The oxide was then washed with NaOH at pH 10.4 and a conductivity value of  $0.362 \text{ S m}^{-1}$ , followed by 12  $H_2O$  washings to a final pH of 7.4 and a conductivity value of  $840 \text{ }\mu\text{S m}^{-1}$ . With each wash the sample was agitated overnight on a reciprocating shaker, and separated for 30 min on a RC-5B Sorvall centrifuge (DuPont Co., Wilmington, DE) at  $40000 \times g$  for the acid suspensions, or  $2000 \times g$  for the alkaline suspensions. After centrifuging and discarding the supernatant, the oxide was scraped from the centrifuge tubes and reagitated with fresh solution. Tiny dark spots ( $\approx 1\%$ ) were noticed on the centrifuge tubes, particularly after the acid washings, and were removed from the oxide sample whenever possible. An  $N_2$  atmosphere was maintained at all times, except during the removal of the oxide from the centrifuge tubes.

After the 12  $H_2O$  washings, the sample was again resuspended in  $H_2O$  and used as the stock Al oxide suspension for all experiments. Approximately 1 L of stock solution was prepared and found to have a density of  $84.06 \text{ g L}^{-1}$  and a specific surface area, using ethylene glycol monomethyl ether (EGME), of  $83.1 \text{ m}^2 \text{ g}^{-1}$ . Before the sample was washed, the initial surface area by EGME was  $95.0 \text{ m}^2 \text{ g}^{-1}$ ; this value compared well with the surface area by BET of  $100 \pm 15 \text{ m}^2 \text{ g}^{-1}$  supplied by the manufacturer. The objective of all these washings was to obtain an Al oxide suspension that was free of unknown impurities.

The adsorption behavior of  $H^+$  ions on the Al oxide was determined by mass balance as outlined in the backtitration technique of Schulthess and Sparks (1986). The procedure was modified by adding 5 mL of Al oxide suspension to 30 mL of pH/electrolyte concentration adjusted water. The pH was adjusted with known quantities of either 0.24 M HCl or 0.24 M NaOH; the electrolyte used was NaCl. The total volume on all samples was 35 mL. The exclusion volume was estimated to be 0.145 mL; thus, the total initial aqueous volume was set equal to 34.855 mL for the backtitration technique calculations. Another run was made with 15 mL of Al oxide suspension and 20 mL of pH adjusted water, with no salt additions. After equilibrating overnight, centrifuging, and filtering through 0.2- $\mu\text{m}$  GA-8 Gelman filter paper, the weighed supernatant was backtitrated to pH 8.00 with either 0.03 M NaOH or 0.03 M HCl.

Prior to backtitrating, some samples were analyzed for  $Cl^-$  or  $Na^+$  concentration remaining in solution. The  $Cl^-$  ion concentration was analyzed with an Orion  $Cl^-$  ion selective electrode; the  $Na^+$  ion concentration was analyzed on a Perkin Elmer 5000 Atomic Absorption spectrometer buffered with LiCl to minimize flame induced ionization problems.

## MODEL DEVELOPMENT

There are two aspects to a model: (i) a physical interpretation, and (ii) a mathematical interpretation. The physical model is intended to help conceptualize the effects exerted on the oxide's surface. The mathematical model is usually the core of the discussion, and it is based here entirely on mass balanced equations. The assumed parameters controlling the transitions of one surface structure to another (mathematical aspect) are independent of the assumptions on what the surface structure actually looks like (physical aspect).

### Basis for a Two-site Model

The more types of sites that are assumed in a model, the greater the number of mathematical parameters available for controlling the behavior of predicted values. However, it is essential that a model, and each of the mathematical parameters, have a physical counterpart to maintain meaning and correspondence with reality. The emphasis here is therefore placed on the chemical nature of Al. With a valence of +3, each edge Al can support two amphoteric surface-OH groups and still remain bonded to the solid phase. For Al, a model involving more than two sites per surface Al atom would be difficult to conceptualize.

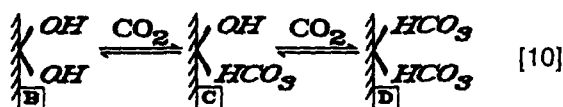
### Determination of $\Gamma_{\max}$

Two values are needed in determining the maximum amount of ions each site can adsorb: the total number of protons adsorbed at the extreme pH values,  $\Gamma_{\text{TOTAL}}$ , and the amount adsorbed to reach an assumed neutral condition,  $\Gamma_0$ . The backtitration technique in proton isotherm analysis of an oxide should show a clear maximum amount of adsorbed  $\text{H}^+$  at very low pH values, or a maximum amount desorbed at very high pH values. At high pH, negative adsorption values denote either  $\text{OH}^-$  adsorbed, or  $\text{H}^+$  desorbed. Electrokinetic studies reviewed by Parks (1965) give ZPC values of 8.0 for Al oxides. With  $\Gamma_0$  as the value obtained at pH 8.0, the maximum amount sorbed per site,  $\Gamma_{\max}$ , is

$$\Gamma_{\max} = \frac{\Gamma_{\text{TOTAL}} - \Gamma_0}{\text{no. of site types}} \quad [9]$$

### $\text{CO}_2$ Adsorption

Even with the precautions taken in using an ultrapure ion exchange cartridge and  $\text{N}_2$  gas during the oxide washings to purge  $\text{CO}_2$  from the system,  $\text{CO}_2$  would still be able to adsorb on the oxide during the brief transfers from the centrifuge tubes, particularly at high pH values. Martin and Smart (1987) observed through x-ray photoelectron spectroscopy (XPS) that C contamination existed on all the goethite ( $\alpha\text{-FeOOH}$ ) surfaces that were exposed to air. The presence of  $\text{CO}_2(\text{aq})$  in the system is therefore considered an active species that can adsorb/desorb from the solid phase. Though the authors were not able to obtain literature on  $\text{CO}_2$  adsorption on Al oxides, the following model was assumed

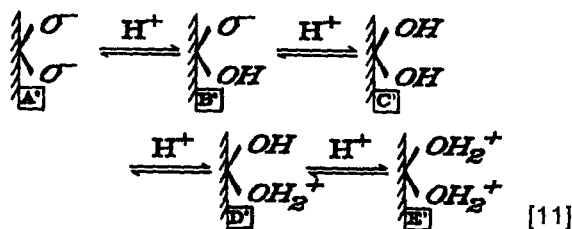


In a closed system, species B would exist at a higher pH than C or D. Higher  $\text{CO}_2(\text{aq})$  concentrations would be expected at lower pH values in a closed system (Stumm and Morgan, 1981), which would in turn increase equilibrium towards  $\text{CO}_2$  adsorption on the Al surface. In an open system,  $\text{CO}_2(\text{aq})$  concentration would be constant and pH in-

dependent (Stumm and Morgan, 1981). Caution should be taken not to confuse  $\text{CO}_2(\text{aq})$  with total carbon,  $(\text{CO}_2)_{\text{TOTAL}} = (\text{H}_2\text{CO}_3) + (\text{HCO}_3^-) + (\text{CO}_3^{2-}) + (\text{CO}_2)_{\text{aq}}$ .

### pH Dependent Reactions: Effects and Limitations

The adsorption and desorption of  $\text{H}^+$  ions on a two-site model may be depicted by



Species A' would exist at very high pH values, C' at the pH of ZPC, and E' at very low pH values. To model Eq. [11], four equilibrium constants (K) and a mass balance condition are needed. The pK values ( $-\log K$ ) used are determined by fitting the curve to the data with no initial NaCl additions. Four plateaus are generated by this model, and the center of each plateau corresponds to 50% of each species involved in the transition. The pK value for each transition controls the location of only one of the plateaus, moving it up or down like elevators. This type of model does not have a parameter that would allow the predictions to vary with changes in the initial electrolyte concentration; i.e., only one line can be generated when plotting adsorption vs. pH.

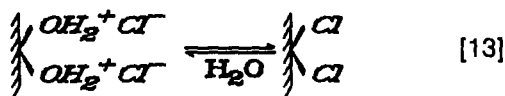
### pH + Salt Dependent Reactions

The positive and negative charges that develop on the oxide surface shown on Eq. [11] are balanced by counterions in the bulk solution. However, if the adsorption of counterions is stoichiometrically related to the adsorption of protons, then there is sufficient reason to incorporate the concentration of the counterions into the model; specifically, in the definition of the equilibrium constants. With the assumption that each transition is dependent on the pH and salt concentration of the bulk solution, the model then would generate a different line for each initial salt concentration when plotting adsorption vs. pH. Again, the pK value for each transition controls the location of one of the plateaus. The assumed equilibrium constants were

$$\begin{aligned} \text{high pH, } K_a &= \frac{[\text{SOH}][\text{OH}^-](\text{Na}^+)}{[\text{SONa}]}, \\ K_b &= \frac{[\text{SHCO}_3](\text{OH}^-)^2}{[\text{SOH}]}, \\ \text{low pH, } K_c &= \frac{[\text{SHCO}_3](\text{H}^+)(\text{Cl}^-)}{[\text{SCL}]} \quad [12] \end{aligned}$$

These reactions may be explained as two simultaneous steps. At high pH, the  $\text{OH}^-$  anion neutralizes the surface-OH proton forming  $\text{H}_2\text{O}$  and a negative surface, and the  $\text{Na}^+$  cation satisfies the charge imbalance. Similarly, at low pH, the  $\text{H}^+$  cation reacts with the surface- $\text{HCO}_3$  group to form  $\text{H}_2\text{CO}_3$  and a positive surface, and the  $\text{Cl}^-$  anion satisfies the charge imbalance. For the surface- $\text{HCO}_3$  group, the transitions shown in Eq. [10] are also assumed to involve two-step reactions, with the surface- $\text{HCO}_3$  to surface- $\text{OH}$  transition resulting in two  $\text{OH}^-$  anions removed from the bulk solution.

It is worthwhile to note that the following two species cannot be differentiated by the potentiometric methods used



The oxide surface on the right is the one used in this paper since it emphasizes that the  $\text{Cl}^-$  anion is an active species in the surface reactions.

### Competitive Salt (pH-independent) Reactions

A set of exchange reactions may also be assumed based on the salt concentrations only, with secondary neutralizing reactions taking place in the bulk solution. For example, a  $\text{Cl}^-$  anion may exchange with a surface-OH (or  $-\text{HCO}_3^-$ ) group, with the reaction dependent only on the  $\text{Cl}^-$  concentration. The exchanged  $\text{OH}^-$  (or  $\text{HCO}_3^-$ ) would in turn consume  $\text{H}^+$  ions in the bulk solution. Similarly, the  $\text{Na}^+$  cation may exchange with the proton of a surface-OH group. The  $\text{HCO}_3^-$  and  $\text{CO}_2(\text{aq})$  concentrations were ignored in all of the competitive reactions; the reactions were assumed to be dependent on  $\text{Na}^+$  or  $\text{Cl}^-$  concentrations only. The assumed equilibrium constants were

$$\begin{aligned} K_d &= \frac{[\text{SOH}](\text{Na}^+)}{[\text{SONa}]}, \text{ and} \\ K_e &= \frac{[\text{SHCO}_3](\text{Cl}^-)}{[\text{SCI}]} \end{aligned} \quad [14]$$

A reaction that consumes (or releases)  $\text{H}^+$  ions in the bulk solution should also be pH dependent. However, the data obtained by the backtitration technique is a result of two reactions: first there is the titration-induced aqueous/surface reactions, followed by the aqueous backtitration reactions. Equation [14] describes the equilibrium constant for those reactions that have had the pH-dependent characteristics presumably factored out by the backtitration procedure. Equation [12] describes the equilibrium constant for those reactions that have remained both pH and salt dependent after the backtitration procedure.

The equilibrium constants described by Eq. [14] generate vertical lines, or pH-independent values, on proton adsorption vs. pH plot analyses. Changes in the salt concentrations result in changes in the amount of  $\text{H}^+$  consumed in the bulk solution (which cannot be distinguished from  $\text{H}^+$  adsorbed on the surface). The pK values for these transitions control the sensitivity of the reaction response to changes in the salt concentrations.

## APPLICATION OF MODEL

### Stoichiometric Considerations

Figure 1 shows the adsorption isotherms of  $\text{H}^+$ ,  $\text{Na}^+$ , and  $\text{Cl}^-$  ions for the samples with 0.0 and 0.001 M initial NaCl concentrations. The isotherms were determined by mass balance (Eq. [8]) and by the backtitration technique (Schulthess and Sparks, 1986). Similar patterns were obtained at higher initial electrolyte concentrations; however, the scatter on the  $\text{Cl}^-$  isotherm was greatly increased due to the difficulty in detecting very small concentration differences at high electrolyte concentrations. The  $\text{Na}^+$  cation was removed from solution at  $\text{pH} > 10$ , and correlates well with the  $\text{H}^+$  desorption pattern. However, at  $\text{pH} > 11.8$  the  $\text{Na}^+$  ion removal was too large and follows a convex pattern. This suggested an error in the determination of  $\text{Na}^+$  ions in the bulk solution. It was hypothesized that the  $\text{Na}^+(\text{aq})$  complexed with the dissolved  $\text{Al}(\text{OH})_2^-(\text{aq})$  and thus avoided detection by atomic absorption spectroscopy. This would cause the

recovered  $\text{Na}^+$  concentration to be underestimated. It was immediately noticed that these independent measurements yield nearly identical results, particularly the  $\text{Cl}^-$  isotherm and the  $\text{H}^+$  isotherm. These observations were central to the development and application of the model in that they established a 1:1 correlation between the salt and  $\text{H}^+$  ion removal from solution. It therefore follows that the model should not only predict the  $\text{H}^+$  isotherm, but also the removal of salt ions from solution.

### Determination of $\Gamma_{\text{max}}$

Figure 2 shows the proton isotherm for the samples containing 1.2609 g of Al oxide with a maximum at  $3.15 \mu\text{mol m}^{-2}$  of  $\text{H}^+$  adsorbed ( $\Gamma_{\text{TOTAL}}$ ) at the low pH values. At the high pH values the maximum is not distinct, and it appears that  $\text{H}^+$  ions may still be released at higher pH values. There is definitely no convex shape to these curves. The isotherm is shifted by  $-0.25 \mu\text{mol m}^{-2}$  ( $\Gamma_0$ ) at pH 8.0, and Eq. [9] gives a displacement of  $3.4 \mu\text{mol m}^{-2}$  ( $= \Gamma_{\text{TOTAL}} - \Gamma_0$ ). A two-site model, therefore, yields a maximum amount of adsorption per site ( $\Gamma_{\text{max}}$ ) of  $1.7 \mu\text{mol m}^{-2}$ . This is equivalent to  $0.977 \text{ nm}^2 \text{ site}^{-1}$  of surface Al containing two active site types of  $0.488 \text{ nm}^2$  each.

### Determination of pK Values

Based on the results shown in Fig. 1, it was assumed that all surface reactions must involve a  $\text{Cl}^-$  anion (or  $\text{Na}^+$  cation), and thus the ion concentration was incorporated in the equilibrium equations. The  $\text{Cl}^-$  and  $\text{Na}^+$  concentrations used in the equations were calculated from the sum of the constituent sources:

$$(\text{Cl}^-)_{\text{eq}} = (\text{NaCl})_{\text{added}} + (\text{HCl})_{\text{added}} - (\text{Cl}^-)_{\text{adsorbed}} \quad [15]$$

$$\begin{aligned} (\text{Na}^+)_{\text{eq}} &= (\text{NaCl})_{\text{added}} + (\text{NaOH})_{\text{added}} \\ &\quad - (\text{Na}^+)_{\text{adsorbed}} \end{aligned} \quad [16]$$

The loss due to adsorption is determined by an iteration procedure. It is important to note that it is impossible to add  $\text{H}^+$  cations without  $\text{Cl}^-$  anions (conjugate base), or  $\text{OH}^-$  anions without  $\text{Na}^+$  cations (conjugate acid). Thus, to generate a prediction on the amount of protons adsorbed at a given pH, the amount of acid or base added had to be known. If no data were available at a given pH, the trapezoidal rule was applied to estimate the amount that would be added. The concentrations were expressed as activities; the ion activity coefficients ( $\gamma$ ) were determined with the Güntelberg equation (Stumm and Morgan, 1981):

$$\log \gamma = \frac{-0.5z^2\sqrt{I}}{1 + \sqrt{I}} \quad [17]$$

where  $I$  = ionic strength, and  $z$  = valence of the ion.

The assumed pH+salt dependent reactions are illustrated vertically in Fig. 3, and the corresponding equilibrium constants are assumed to be dependent on one pH term ( $\text{H}^+$  or  $\text{OH}^-$ ), and one salt term ( $\text{Na}^+$  or  $\text{Cl}^-$ , but may also be  $\text{OH}^-$  again); see Table 1 for definitions of  $K_1$  to  $K_5$ . The transitions  $B \rightleftharpoons C \rightleftharpoons D$  (Fig. 3) are presumed to consume  $\text{H}^+$  ions only in the bulk solution. This gives one  $\text{H}^+$  desorbed for each species  $A$  formed, one  $\text{H}^+$  adsorbed for each species

*E* formed, and two  $H^+$  adsorbed for each species *F* formed. Likewise for the  $Cl^-$  anion, species *E* and *F* correspond to one and two  $Cl^-$  adsorbed, respectively. Each  $pK$  value (Table 1, [1]-[5]) was determined one

at a time and all the other reactions were ignored. These  $pK$  values control the location of the plateaus, and the values were chosen based on the best fit of the curve corresponding to the data with no initial

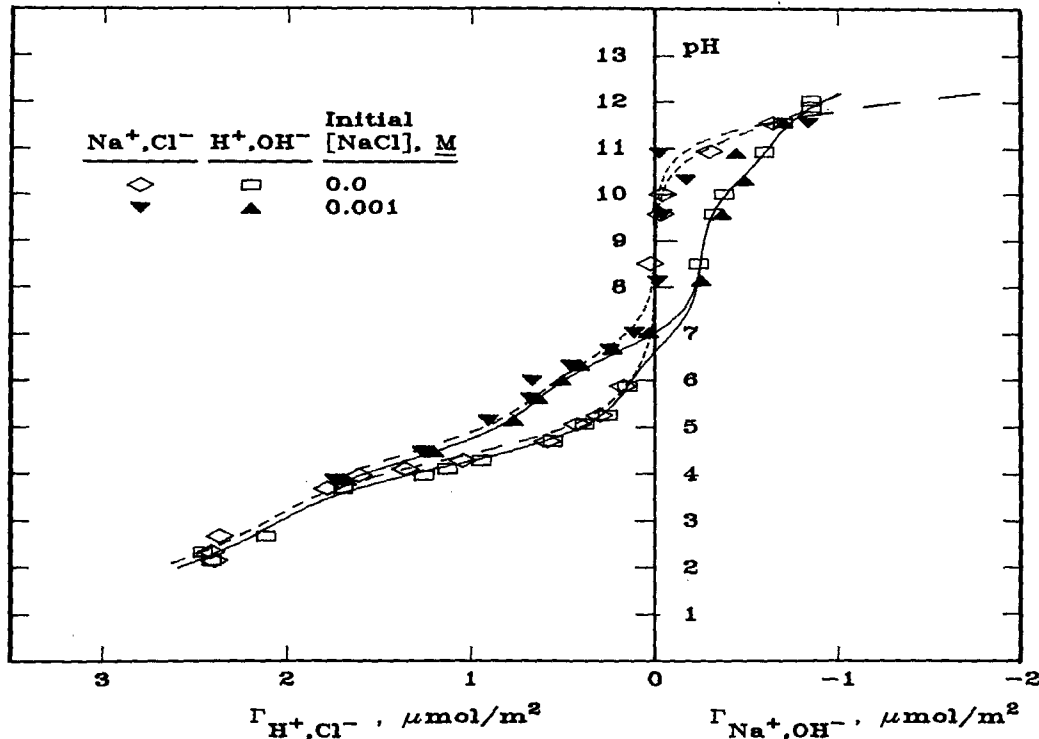


Fig. 1. Adsorption isotherm on Al oxide: (□) proton adsorption with no initial NaCl additions; (▲) proton adsorption with 0.001 M NaCl added; (◇)  $Cl^-$  ion adsorption ( $pH < 8$ ), or  $Na^+$  cation adsorption ( $pH > 8$ ), with no initial NaCl additions; (▽)  $Cl^-$  ion adsorption ( $pH < 8$ ), or  $Na^+$  cation adsorption ( $pH > 8$ ), with 0.001 M NaCl added. Proton isotherms traced with solid lines;  $Na^+$  and  $Cl^-$  isotherms traced with dashed lines.

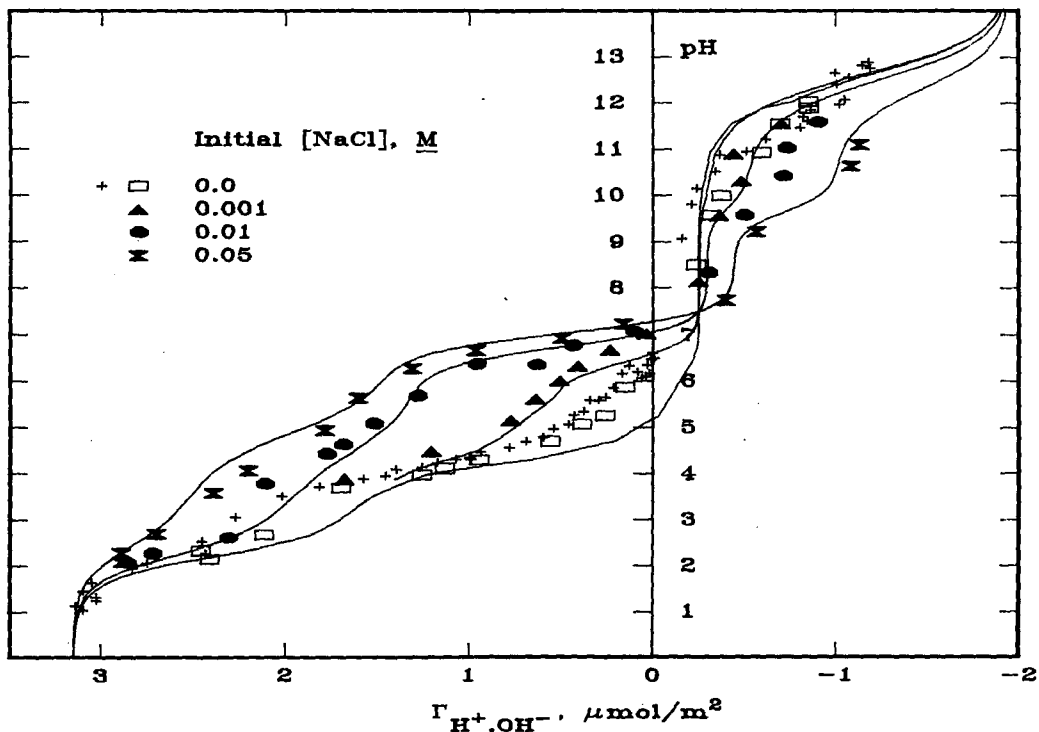


Fig. 2. Proton adsorption isotherm on Al oxide with predicted values of  $pH$ +salt/salt-competitive model shown by solid line (impurities ignored). Symbols (+) correspond to samples with 1.2609 g of Al oxide; all other symbols correspond to samples with 0.4203 g of Al oxide.

NaCl additions. The resulting curves (not shown) greatly underestimated the data for high electrolyte concentrations, but this was to be expected without the incorporation of the salt-dependent reactions.

By studying the data shown in Fig. 2, it becomes apparent that there must also be a pH-independent reaction involved in the model. It is easy to see the pH-dependent behavior (proton adsorption not present at high pH, and proton desorption not present at low pH), but a pH-independent behavior is also shown. In Fig. 2, between pH 5 and 7, there are adsorption maxima reached whose values depend on the salt concentration present. The same thing is observed in various parts of the graph: between pH 2 and 3, 8 and 9, and 10 and 11. Therefore, competitive pH-independent reactions have been introduced into the model. The hypothesized reactions are shown in Fig. 3 with the pH + salt-dependent reactions drawn vertically and the pH-independent reactions drawn horizontally.

Table 1. The equilibrium constants for the reactions illustrated in Fig. 3 ( $pK = -\log K$ ).†

Equilibrium constants	pK	Reaction no.
$K_1 = \frac{\{A\}}{\{B\}(Na^+)(OH^-)}$	-3.2	[1]
$K_2 = \frac{\{B\}}{\{C\}(OH^-)^2}$	-8.5	[2]
$K_3 = \frac{\{C\}}{\{D\}(OH^-)^2}$	-15.5	[3]
$K_4 = \frac{\{D\}(H^+)(Cl^-)}{\{E\}}$	7.5	[4]
$K_5 = \frac{\{E\}(H^+)(Cl^-)}{\{F\}}$	4.2	[5]
$K_6 = \frac{\{G\}}{\{H\}(OH^-)^2}$	-8.5	[6]
$K_7 = \frac{\{B\}(Na^+)}{\{G\}}$	1.2	[7]
$K_8 = \frac{\{C\}(Na^+)}{\{H\}}$	0.5	[8]
$K_9 = \frac{\{D\}(Cl^-)}{\{I\}}$	3.0	[9]
$K_{10} = \frac{\{E\}(Cl^-)}{\{J\}}$	1.6	[10]
$K_{11} = \frac{\{B\}(M^+)}{\{M\}}$	2.8	[11]

† Braces  $\{i\}$  are activity of surface species  $i$  shown in boxes next to corresponding oxide surface in Fig. 3. Parentheses  $(i)$  are activity of species  $i$  in bulk solution. The subscripts correspond to reaction numbers shown in boxes in Fig. 3.

The pK values for the salt-dependent reactions were also determined one at a time; the pH + salt-dependent reactions and their respective pK values previously determined were not ignored. For the pH range 5 to 7, the hypothesized  $Cl^-$  anion dependent reaction (Table 1, [9]) is essentially a substitution reaction of  $Cl^-$  for  $HCO_3^-$ . The pK<sub>9</sub> value was calculated based on the best fit of the data. The same procedure and hypothesis were applied for the pH range 2 to 3 (Table 1, [10]). For the pH range 8 to 9, and 10 to 11, the competitive  $Na^+$  ion dependent reactions are assumed to be substitution reactions of  $Na^+$  for  $H^+$ . These pK values (Table 1, [7]–[8]) were determined by the best fit with the high initial NaCl concentration data. An important observation was made in trying to fit the alkaline data: The competitive products must be interconnected by pH + salt-dependent reactions. Without these connections (Table 1, [6]) the predicted values would reverse themselves. For example, if Reaction [6] is ignored, then the model would predict proton desorption at pH > 8 (due to some formation of species  $H$ ), proton desorption reversal at pH > 8.5 (due to formation of neutral species  $B$ , and depletion of species  $H$ ), followed by proton desorption at pH > 9.5 (due to some formation of species  $G$ ). These reversals do not occur as long as the competitive products are connected. Since these pK values cannot be fitted, they are assumed to be identical to the paralleled reactions; e.g.,  $pK_6 = pK_2$ .

The solid lines drawn in Fig. 2 show the predictions generated based on the pK values defined in Table 1 for the pH + salt/salt-dependent reactions just described.

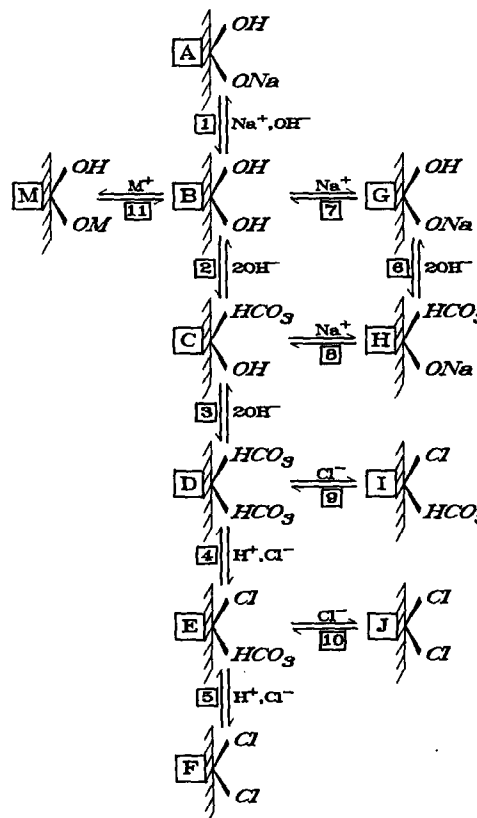


Fig. 3. The competitive pH + salt/salt-dependent reactions.

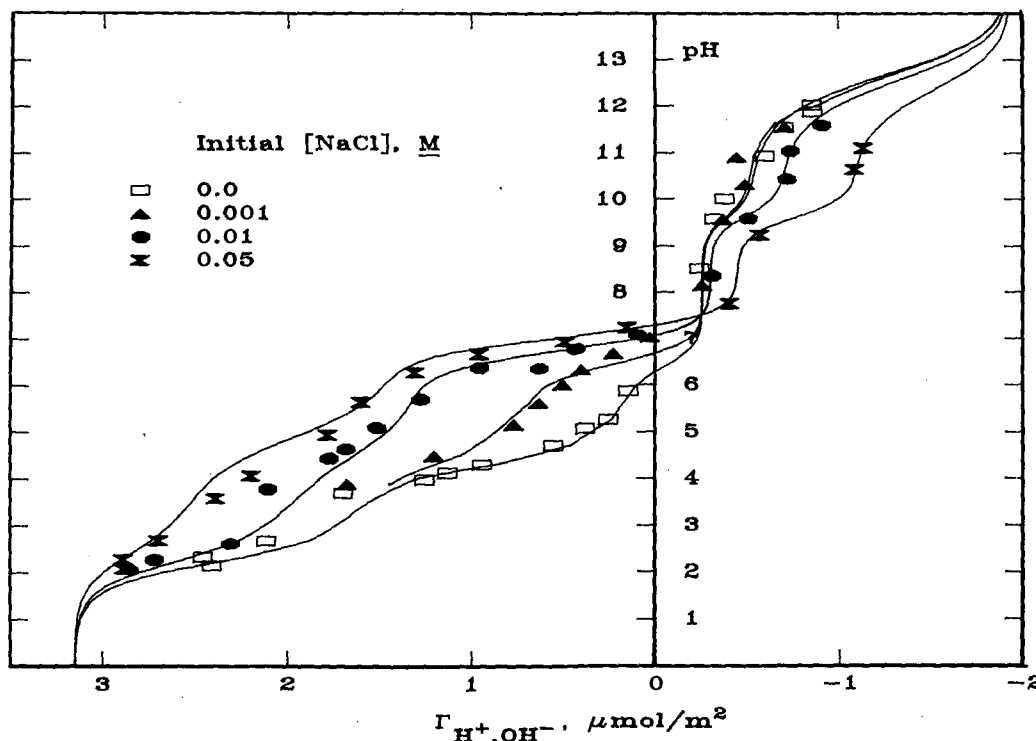


Fig. 4. Proton adsorption isotherm on Al oxide determined by the backtitration technique for several initial NaCl concentrations. The lines drawn are the predicted values of the pH+salt/salt-competitive model.

#### The Adsorption Shift: Impurity Effects

In Fig. 2, for the data with no NaCl additions, the model underestimates the amount of protons adsorbed in the slightly acidic pH range (5–7). To understand this discrepancy, note that the isotherm data for washed Al oxide differ from the unwashed Al oxide data previously reported (Schulthess and Sparks, 1986), particularly with respect to the amount of shift of the PZSE from the zero adsorption readings. Since the washings narrowed the amount of shift, it was assumed that any shift observed was due to initial salt impurities still remaining on the oxide surface after washing. The source of the salt may be from the oxide lattice itself, as well as from the product of the acid followed by base washings.

The Al oxide was manufactured by flame hydrolysis of anhydrous  $\text{AlCl}_3$ . The Degussa product quality control indicates <0.5% HCl may be present. For this reason,  $\text{Cl}^-$  anions are the presumed impurity that causes the negative PZSE shift. This is in contradiction with Huang (1981), who states that negative PZSE shifts are due to specific cation adsorption. However, assuming an initial  $\text{Cl}^-$  concentration of 0.0005 M due to impurities (determined by a best fit analysis), the model predictions are almost on target with all the data in the acidic range (Fig. 4).

In Fig. 2, the model also underestimates the amount of proton desorbed in the alkaline pH region (>9.5). Again, the reasoning is based on salt impurities. However, there is no information as to what kind of cation may be present as an impurity. For the low initial NaCl additions, the model shown in Fig. 2 underestimates the data by an amount nearly equal to the PZSE shift. It was therefore assumed that the amount

of cation ( $\text{M}^+$ ) impurity present was equivalent to the amount of anion ( $\text{Cl}^-$ ) impurity assumed earlier (0.0005 M). The  $\text{M}^+$  cation may be related to the tiny dark spots observed during the washings.

Figure 3 illustrates the  $\text{M}^+$  cation competing with the pH+salt-dependent reactions, just like the  $\text{Na}^+$  cation. The  $\text{p}K$  value for this competitive metal reaction was determined by best fit of the data, and is shown in Fig. 4.

#### Overview: Speciation of Surface

The proton isotherm shown in Fig. 4 was modeled based on the observations of five plateaus corresponding to five pH+salt-dependent reactions, and four adsorption shifts corresponding to four competitive salt-dependent reactions. Mathematical modeling of the reactions illustrated in Fig. 3 was based on the equilibrium constants shown in Table 1, and the following mass balance condition:

$$\{A\}_{\text{TOTAL}} = \{A\} + \{B\} + \{C\} + \{D\} + \{E\} + \{F\} + \{G\} + \{H\} + \{I\} + \{J\} + \{M\}. \quad [18]$$

Each species was defined in terms of a common species with the equilibrium constants in Table 1. The speciation fraction,  $\alpha_i$ , for each species was defined as the ratio  $\Gamma_i/\Gamma_{\text{max}}$  by

$$\alpha_i = n_i/D \quad [19]$$

where  $D = \sum n_i$ , and the  $n_i$  values defined in Table 2. Note that  $\sum \alpha_i \equiv 1.0$ , and each surface speciation fraction may be independently determined given only the pH and the equilibrium salt concentration (Eq. [15]–[16]). The model finally predicts the proton adsorption isotherm by

Table 2. Numerator values,  $n_i$ , for determining surface speciation fractions,  $\alpha_i$ .

$n_A = K_1 K_2 K_3 (\text{Na}^+) (\text{OH}^-)^5$	$n_H = \frac{K_3 (\text{Na}^+) (\text{OH}^-)^2}{K_8}$
$n_B = K_2 K_3 (\text{OH}^-)^4$	
$n_C = K_3 (\text{OH}^-)^2$	$n_I = \frac{(\text{Cl}^-)}{K_9}$
$n_D = 1$	
$n_E = \frac{(\text{H}^+) (\text{Cl}^-)}{K_4}$	$n_J = \frac{(\text{H}^+) (\text{Cl}^-)^2}{K_4 K_{10}}$
$n_F = \frac{(\text{H}^+)^2 (\text{Cl}^-)^2}{K_4 K_6}$	$n_M = \frac{K_2 K_3 (\text{M}^+) (\text{OH}^-)^4}{K_{11}}$
$n_G = \left( \frac{K_6 K_3}{K_8} + \frac{K_2 K_3}{K_7} \right) (\text{Na}^+) (\text{OH}^-)^4$	

$$\Gamma_{\text{H}^+, \text{OH}^-} = \Gamma_{\text{max}} (\alpha_I + \alpha_E + 2\alpha_J + 2\alpha_F - \alpha_A - \alpha_G - \alpha_H - \alpha_M) + (\text{Shift}) \quad [20]$$

where  $\Gamma_{\text{max}} = 1.7 \mu\text{mol m}^{-2}$ , and  $\text{Shift} = -0.25 \mu\text{mol m}^{-2}$ . It should be emphasized that the data were not force fitted. Force fitting involves at least one independent empirical parameter that cannot be experimentally determined. All the pK values were obtained by best fit with the data, but there were no empirical parameters involved. All concentration values used in the model were experimentally confirmed. An exception is the  $(\text{M}^+ \text{Cl}^-)$  impurity concentration, which may be improved upon in future model revisions. The existence of the  $\text{M}^+ \text{Cl}^-$  impurity, however, is strongly suggested by the visual observation, the manufacturing procedure, and by the decrease in the amount of shift of the PZSE from the zero adsorption readings after washing the oxide.

Figure 5 shows the speciation of the Al oxide surface for various initial electrolyte concentrations as a function of pH. Species  $M$ ,  $A$ ,  $G$ , and  $H$  all consume one  $\text{OH}^-$  anion, and are summed under the  $-1$  curve in Fig. 5. Species  $B$ ,  $C$ , and  $D$  are neutral, and are summed under the 0 curve. Species  $I$  and  $E$  consume one  $\text{H}^+$  ion, and are summed under the  $+1$  curve. Finally, species  $J$  and  $F$  consume two  $\text{H}^+$  ions and are summed under the  $+2$  curve. The removal of  $\text{Na}^+$  cations are also summed under the  $-1$  curve, and the removal of  $\text{Cl}^-$  anions are also summed under the  $+1$  and  $+2$  curves. Two vertical lines are drawn in Fig. 5 that indicate the pH of two surface conditions: negative = positive surface concentration, and maximum concentration of neutral surface sites. The former always occurred at lower pH values than the latter.

## RESULTS AND DISCUSSION

The intersection of the curves in Fig. 4 at pH 7.5 is the PZSE, and Fig. 5 shows that it coincides with the surface condition of  $\text{H}^+$  adsorption equivalent to  $\text{H}^+$  desorption (or,  $\text{H}^+$  consumed =  $\text{OH}^-$  consumed). Technically, Fig. 5 shows that the PZSE decreases with increasing electrolyte concentration (7.76–7.50). However, in Fig. 4 it is the high ionic strength (I) curves that are visibly seen intersecting the other curves at

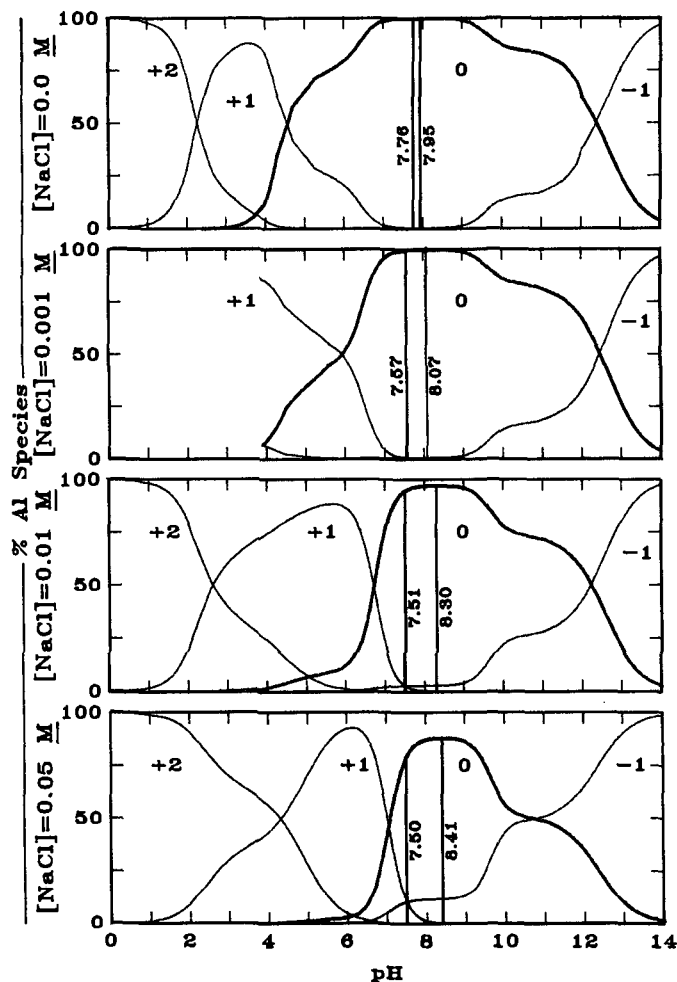


Fig. 5. The surface speciation of the Al oxide.

pH 7.50 (or, at the pH of PZSE for the high I curves). The amount of  $\text{Cl}^-$  adsorbed is also equivalent to the amount of  $\text{Na}^+$  adsorbed at the PZSE, based on Fig. 1 and on the stoichiometric relationship assumed in the proposed model. It is emphasized that the proton isotherm, and the cation and anion isotherms, are stoichiometrically related. The term *point of zero net charge* (PZNC) has been suggested for the condition of cation exchange capacity = anion exchange capacity ( $\text{CEC} = \text{AEC}$ ) (Sposito, 1984), and would therefore be equivalent to the PZSE; i.e., these two independently measured isotherms should agree on their respective neutral values or intersection points.

Figure 5 also shows that the maximum concentration of neutral surface sites falls at pH values  $>$  pH of PZSE (pH range 7.95–8.41, depending on the NaCl concentration). This emphasizes that *neutral surface conditions* are not equivalent to *maximum concentration of neutral sites*. The difference between them increases with the electrolyte concentration of the analysis.

A ZPC analysis (not shown) of this washed Al oxide, using traditional potentiometric methods (Schulthess and Sparks, 1986), showed an intersection of the isotherms at pH 7.5. The reference used for this analysis was theoretical (singular reference curve method) and the pH plotted was the supernatant pH. It was also

observed that since the data tend to be in close proximity between pH 7 and 9, it is easy to misplace the ZPC value by as much as one pH unit. Thus, if sufficient data are collected near the pH of neutral surface conditions, the ZPC values obtained by singular reference curve methods are similar to the PZSE values obtained by the backtitration method. The advantages of the backtitration technique are primarily on the analyses of the proton isotherm. It is not clear at this time if the PZSE and ZPC values would agree in systems with multiple surface sites; this uncertainty is due to the variable solubility of each surface present.

The concept of competitive behavior also suggests that anion adsorption envelopes (Hingston et al., 1967, 1972) are merely an adsorption competition between the anion studied with all the other anions in the system. One should keep in mind that as acidic  $H^+$  ions are added, anions are also added. The anion specificity is pH-dependent due to the competitive behavior of  $OH^-$  anions. If the anions in solution vary with pH, then the model is obviously more complex. However, for an anion such as  $F^-$ , the adsorption pattern is competing with  $OH^-$  anions at high pH values (right side of adsorption envelope), and also competing with  $Cl^-$  anions added as HCl at low pH values (left side of adsorption envelope). The presence of  $CO_2(aq)$  may also complicate any proposed model. Therefore, it is strongly recommended that if pH-dependent studies are performed, that the form of the acid or base used be clearly stated, and that the amount used be considered as a significant factor in the experiment.

### CONCLUSIONS

The proton isotherm behavior of an Al oxide can be successfully modeled with mass balanced equations. Intrinsic equilibrium constants and exponential terms were avoided due to an error in the development of these terms. A backtitration technique (Schulthess and Sparks, 1986) was used to collect the proton isotherm data, and was found to be stoichiometrically related to the cation and anion isotherm behavior. The assumed model was based on: (i) two surface sites, (ii) pH + salt-dependent reactions ( $H^+$  and  $Cl^-$ ,  $2OH^-$ , or  $Na^+$  and  $OH^-$ ), (iii) competitive salt dependent reactions ( $Na^+$  or  $Cl^-$ ), (iv)  $CO_2(aq)$  pH-dependent reactions with the surface- $OH$  groups, and (v) presence of an unknown  $M^+Cl^-$  salt (0.0005 M). The total number of Al sites was  $1.7 \mu\text{mol m}^{-2}$  (equivalent to  $0.977 \text{ nm}^2 \text{ site}^{-1}$  of surface Al), or  $3.4 \mu\text{mol m}^{-2}$  of total available sites. Figure 3 shows the assumed physical interpretations of the proposed model. The pH of PZSE represented the surface condition in which the negative charges (or cation surfaces) equaled the positive charges (or anion surfaces); the CEC equaled AEC at this value. The CEC-AEC data and proton isotherm data were stoichiometrically correlated. The pH of PZSE values ranged from 7.50 to 7.76 depending on the electrolyte concentration present, with lower val-

ues as the concentration increased. The initial presence of impurities on the surface studied will cause the intersection of the curves on the proton isotherm analysis to shift from the zero adsorption axis. Negative shifts are due to anion impurities adsorbed on the surface at initial experimental conditions; conversely, positive shifts are due to cation impurities. These theories would also explain the anion adsorption envelope phenomena as the result of competitive anion reactions.

The ZPC intersection of the  $\sigma_o$ -pH curves generated by traditional potentiometric methods, or singular reference curve methods (Schulthess and Sparks, 1986), was found to coincide with the PZSE value of the backtitration method. However, since the singular reference curve methods do not account for the pH-dependent solubility of the surface, their resulting proton isotherms are not representative of the proton adsorption phenomena. The solubility effects greatly overshadow any adsorption phenomena, and it may be the solubility phenomena that is being tracked by the exponential terms in models involving intrinsic equilibrium constants.

### REFERENCES

- Barrow, N.J. 1985. Reaction of anions and cations with variable-charge soils. *Adv. Agron.* 38:183-230.
- Figurovsky, N. 1973. Johann Tobias Lovits (Lowitz). p. 519-520. *In* C.C. Gillispie (ed.) *Dictionary of scientific biography*. Vol. 8. Charles Scribner's Sons, New York.
- Hingston, F.J., R.J. Atkinson, A.M. Posner, and J.P. Quirk. 1967. Specific adsorption of anions. *Nature (London)* 215:1459-1461.
- Hingston, F.J., A.M. Posner, and J.P. Quirk. 1972. Anion adsorption by goethite and gibbsite. I. The role of the proton in determining adsorption envelopes. *J. Soil Sci.* 23:177-192.
- Huang, C.P. 1981. The surface acidity of hydrous solids. p. 183-217. *In* Marc A. Anderson and Alan J. Rubin (ed.) *Adsorption of inorganics at solid-liquid interfaces*. Ann Arbor Science, Ann Arbor, MI.
- Huang, C.P., and W. Stumm. 1973. Specific adsorption of cations on hydrous  $\gamma\text{-Al}_2\text{O}_3$ . *J. Colloid Interface Sci.* 43:409-420.
- Langmuir, I. 1918. The adsorption of gases on plane surfaces of glass, mica and platinum. *J. Am. Chem. Soc.* 40:1361-1403.
- Lyklema, J. 1968. The structure of the electrical double layer on porous surfaces. *J. Electroanal. Chem. Interfacial Electrochem.* 18:341-348.
- Martin, R.R., and R.St.C. Smart. 1987. X-ray photoelectron studies of anion adsorption on goethite. *Soil Sci. Soc. Am. J.* 51:54-56.
- Olsen, S.R., and F.S. Watanabe. 1957. A method to determine a phosphorus adsorption maximum of soils as measured by the Langmuir isotherm. *Soil Sci. Soc. Am. Proc.* 21:144-149.
- Parks, G.A. 1965. The isoelectric points of solid oxides, solid hydroxides, and aqueous hydroxo complex systems. *Chem. Rev.* 65:177-198.
- Romm, E.S., and A.A. Rubashkin. 1985. Theory of the electric double layer on an oxide-electrolyte-solution boundary. *Colloid J. USSR* 47:463-470. (Engl. transl.) *Kolloidn. Zh.* 47:545-552.
- Schulthess, C.P., and D.L. Sparks. 1986. Backtitration technique for proton isotherm modeling of oxide surfaces. *Soil Sci. Soc. Am. J.* 50:1406-1411.
- Sposito, G. 1983. On the surface complexation model of the oxide-aqueous solution interface. *J. Colloid Interface Sci.* 91:329-340.
- Sposito, G. 1984. *The surface chemistry of soils*. Oxford University Press, New York.
- Stumm, W., and J.J. Morgan. 1981. *Aquatic chemistry*. 2nd. ed. John Wiley & Sons, Inc., New York.
- Westall, J., and H. Hohl. 1980. A comparison of electrostatic models for the oxide/solution interface. *Adv. Colloid Interface Sci.* 12:265-294.